

Co-Firing Ramie Residue with Supplementary Coal in a Cyclone Furnace

Qiguo Yi,^{a,b} Fangjie Qi,^a Bo Xiao,^c Zhiquan Hu,^{a,c,*} and Shiming Liu^a

Co-firing ramie residue with coal was carried out in a thermogravimetric analyzer and a cyclone furnace to evaluate the effects of coal fraction (0 to 30 wt. %) on combustion performance. Thermogravimetric analysis (TGA) results showed that devolatilisation was the predominant process when the coal percentage in the blend was below 30 wt. %. For pure biomass firing in the cyclone furnace, an optimum equivalence ratio (ER = 1.16) was found. Coal additions (0 to 30 wt. %) led to less slagging/fouling problems, higher combustion temperature and higher combustion efficiency along with low pollutant emissions, while the improvement in combustion temperature was weakened as the coal blend ratio exceeded 20 wt.%. The maximum temperature in the cyclone furnace increased from 1215 to 1319°C as the coal fraction increased from 0 to 30 wt.%.

Keywords: Biomass; Cyclone furnace; Co-firing; Slagging/fouling; Combustion efficiency

Contact information: a: School of Environmental Science and Engineering, Huazhong University of Science and Technology, Wuhan 430074, PR China; b: Department of Information Engineering, Wuhan University of Technology Huaxia College, Wuhan 430074, PR China; c: State Key Laboratory of Coal Combustion, Huazhong University of Science and Technology, Wuhan 430074, PR China;

* Corresponding author: yqgjoy@163.com, zhiquanhu@yahoo.com.cn

INTRODUCTION

Ramie (*Boehmeria nivea*), also known as “China grass,” is widely cultivated in China for its fiber from its woody stems; it is used as endemic textile raw material. China's production of ramie has accounted for more than 90% of the world-wide production. However, residual decorticated stems amount to approximately 4.5 million tons annually. Conventional methods for disposal of ramie waste include burning in stacks and dumping in landfills, which result in serious environmental pollution and also enormous waste of resources. The reuse of ramie residue as potential bio-energy will be essential.

In recent years, many technologies, such as combustion, pyrolysis, and gasification have been studied for their possible use with agricultural waste. Ramie residue is also used in papermaking, fiberboard manufacture, and ethanol production. Nowadays, combustion is the simplest and most direct technology available for biomass utilization (Dai and Grace 2008). A novel lab-scale cyclone furnace was designed based on biomass micron fuel (BMF) with a particle size of less than 250 μm (Luo *et al.* 2009). Biomass fuels require relatively long residence time in a high-temperature region in order to avoid the escape of high volatile substances. This can be easily achieved by the combustion of BMF in the cyclone furnace due to rotary combustion upwards along the furnace wall. Smaller particle size improves heating and combustion rates of biomass and shortens the

residence time required; the flame stability in the cyclone furnace can be fulfilled with lower equivalence ratio (ER) (Luo *et al.* 2009, 2010).

However, combustion of pure biomass will result in severe problems of slagging and corrosion due to high alkali and chlorine content, which can be effectively controlled by co-firing biomass with coal. Furthermore, coal addition may increase the heating value (Haykiri-Acma and Yaman 2008). Thus, co-firing is an alternative for solving these drawbacks including seasonal shortage of biomass.

Co-firing of biomass together with a base fuel in a boiler is a simple and economically suitable way to replace fossil fuels, which can reduce NO_x, SO_x, and fossil fuel derived CO₂ emissions. In previous studies (Haykiri-Acma and Yaman 2008; Leckner 2007; Munir *et al.* 2009, 2010a, 2010b, 2011; Narayanan and Natarajan 2007; Sami *et al.* 2001; Skodras *et al.* 2002; Tillman 2000; Wang *et al.* 2011) biomass was typically utilized as a secondary fuel; however, it may also be used as a primary fuel in co-combustion with coal (also referred to as 'reverse co-firing'). To the authors' knowledge, very few studies on reverse co-firing have been reported (Madhiyanon *et al.* 2009, 2011; Sathitruangsak *et al.* 2009). In the present study, we examined the feasibility of co-firing ramie residue with coal in the cyclone furnace. The effects of the coal blend ratio (0 to 30 wt. %) on the combustion temperature, slagging/fouling, and fuel gas emissions were investigated.

EXPERIMENTAL

Materials

The feedstock materials of BMF in this work were from ramie residue obtained from a farm in Xianning City, Hubei Province, China. The coal was from Shanxi Province, China. The particle size of the samples was less than 0.250 mm. Ultimate and proximate analyses are presented in Table 1. Tests were carried out with different coal/biomass ratios of 10, 20, and 30% on a mass basis (12.5, 24.3, and 35.5% on an energy basis), respectively. The particles were mixed intensively before firing into the furnace to ensure the homogeneity of the fuel.

Table 1. Ultimate and Proximate Analyses of the Samples

Sample	Ultimate Analysis (wt.%, d)					Proximate Analysis (wt.%, ad)				HHV (MJ/kg)
	C	H	O ^a	N	S	MC	VM	FC ^a	Ash _d	
BMF	49.42 ±0.06	7.82 ±0.02	41.47 ±0.06	0.12 ±0.05	0.06 ±0.008	8.07 ±0.26	76.50 ±1.27	14.41 ±0.57	1.11 ±0.18	19.37 ±0.32
Coal	55.92 ±0.13	3.47 ±0.02	5.34 ±0.14	1.03 ±0.03	1.08 ±0.01	1.26 ±0.10	22.08 ±0.45	43.92 ±0.35	33.16 ±0.49	24.90 ±0.41

d: dry basis; ad: air-dry basis; ^a Calculated by difference.

Thermogravimetric analysis was carried out by TA Instruments system (Diamond TG/DTA, Perkin Elmer Instruments) in an air atmosphere at a heating rate of 20°C/min. from ambient to 800°C. A sample mass of 3.5±0.5 mg was used for each experiment; all the experiments were repeated, and the mean values were used provided that the deviations were within 5%. Although extrapolation of TGA results to other devices at a larger scale cannot be performed directly, the information obtained from the DTG profiles could be used for an initial evaluation of the combustion behaviour on an

industrial scale. This would prove very useful both from a fundamental viewpoint and for the comparison of samples

Apparatus and Procedures

The lab-scale combustor primarily consists of a cyclone furnace, a temperature measurement system, a fuel supply system, and an air supply system (Fig. 1). The tubular furnace made of steel has a length of 3000 mm and an inner diameter (i.d.) of 250 mm. The inner walls are refractory lined over the whole length of the chamber and externally with ceramic fiber. The top is coned shape in order to reduce dust particles in flue gas. To facilitate gas/solid sampling, 18 utility ports are distributed radially along the length of the furnace. The combustor is divided into three cross sections along the chamber and each section is evenly distributed with three thermocouples through the available ports.

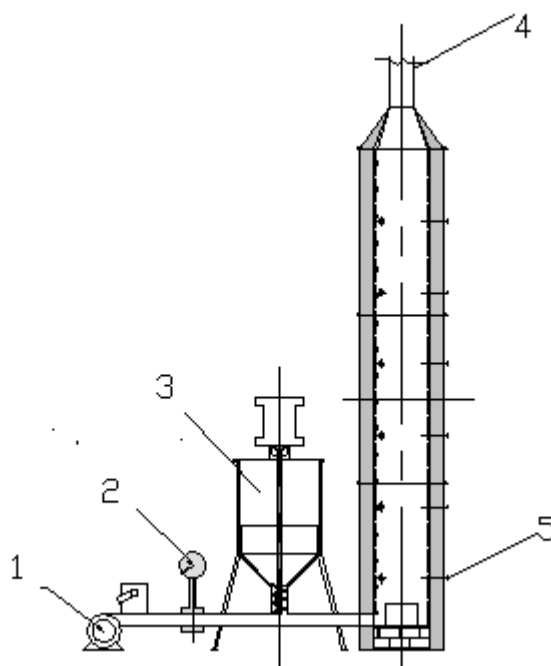


Fig. 1. The structure figure of BMF cyclone combustion system: 1 centrifugal fan; 2 flow meter; 3 screw feeder; 4 chimney; 5 thermocouple

Pulverized fuel (a mixture of BMF and coal) was pneumatically fed tangentially to the furnace wall at the bottom by a high-pressure centrifugal fan and screw feeder. This was intended to simulate the flow pattern in the cyclone furnace. Fuel and air underwent intensive mixing between the screw feeder and cyclone furnace. The feeding rate was controlled by an electric motor. Extensive trial tests were conducted to select reasonable operation conditions in this study. Fuel was added to the screw feeder at the start of each run. The chamber was preheated with coal gas. The ignition temperature of the BMF is about 260°C derived from the TGA above. Therefore, the screw feeder and centrifugal fan were simultaneously started when the temperature at the bottom of the furnace rose above 260°C. The temperatures of each point were recorded by a data logger with an accuracy of $\pm 1^\circ\text{C}$. The exhaust gas was analyzed by a Delta 2000CD-IV gas analyzer. The accuracy of gas (NO_x , SO_x , and CO) measurement was $\pm 5\%$ reading.

The duration of each test run was about 4 h, of which 0.5 h was used to achieve steady state. Steady state was determined by temperature and exit O_2 level. After steady

state was reached, flue gas concentrations were monitored every 10 min for a 2 h period. Each experiment was repeated three times. The data reported in this study are average value of the replicates, and the relative standard deviation was within 10%. The overall thermal input to the combustor was fixed at 160 kW. The effect of coal blend ratios (0 to 30 wt. %) on combustion performance was investigated for the optimum equivalence ratio (ER).

RESULTS AND DISCUSSION

Thermal Characteristics of the Samples under Air Atmosphere

The mass loss (TG) and derivative (DTG) curves of the samples are presented as a function of temperature in Fig. 2.

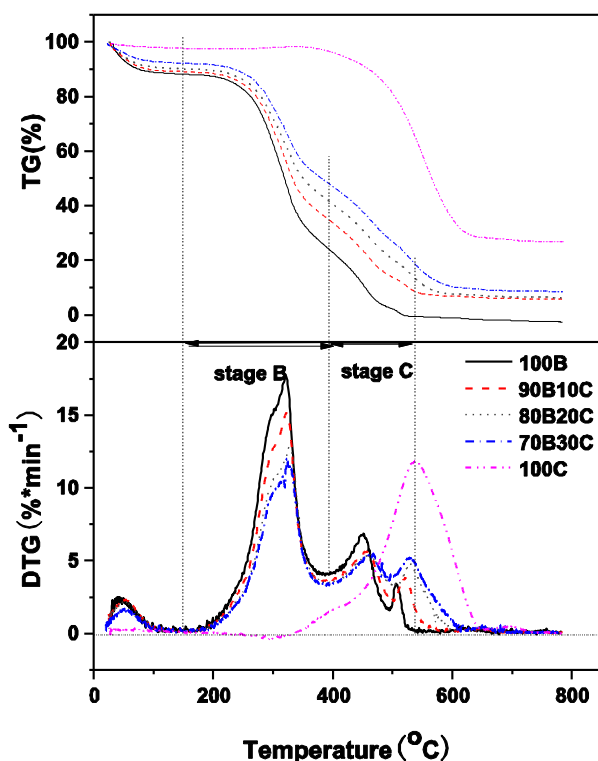


Fig. 2. TG and DTG curves of the samples at different coal blend ratio

An initial mass loss occurred between the temperatures of 25 and 135°C for all samples, due to moisture evaporation. After that, the combustion of the BMF is divided into two stages (Gil *et al.* 2010): oxidative degradation (stage B) and char combustion (stage C). Stage B, which occurred from 135 to 390°C, corresponded to the release and combustion of volatile compounds generated during the decomposition of hemicellulose and cellulose, along with some decomposition of lignin. In stage C (390 to 527°C), the remaining lignin is decomposed and the char residues are combusted. As suggested by Jeguirim *et al.* (2010), the second stage of mass loss was attributed to the fast combustion of reactive combustibles and the slow oxidation of the less reactive combustible part.

However, the DTG curve for coal had one overlapping peak at 536°C and a shoulder section. Contrary to the results found by Li *et al.* (2011), the fixed carbon in the ramie residue burnt faster than that of coal. This observation may be due to the lower ash content in the ramie residue than that in the tobacco residue. Moreover, increasing the coal fraction tended to slightly delay thermal degradation processes towards higher temperatures at stage B. Meanwhile, the volatility causing early release of a significant quantity of volatiles promoted early ignition of the mass of fuel. Thus, the blend burning started earlier than pure coal, which enhanced the thermal reactivity of coal. In contrast, at stage C, the maximum rate of mass loss increased with an increase of the coal blend ratio, indicating that the higher amount of coal in the blend resulted in faster mass loss at a high temperature. This is due to the fact that coal had a higher carbon content, which enhanced the combustion of the char at the high temperature stage. The volatiles burned rapidly at a low coal fraction (0 to 30% by mass) in blends. The higher VM content of the biomass can also result in a highly porous char, thus accelerating the char combustion (Tillman 2000). Overall, devolatilisation was the predominant process when the coal percentage in the blend was below 30 wt. %.

Effect of Coal Blend Ratio on Combustion Temperature and Combustion Efficiency

In order to compare the effects of coal addition, tests of only biomass firing while keeping the optimum ER were taken as the baseline. The combustion efficiency at each run can be calculated according to the CO and the CO₂ emissions in flue gas, and the unburned carbon in ash. The unburned carbon in the fly ash and the bottom ash was quite limited when burning the BMF in the cyclone furnace; thus, the combustion efficiency was mainly determined by the concentration of CO and CO₂ in flue gas as follows:

$$eff = \frac{CO_2 [\%]}{CO [\%] + CO_2 [\%]} \quad (1)$$

Equivalence ratio (ER) is defined as the actually fed air weight divided by the stoichiometrical air weight. ER is a key factor to estimate combustion performance. Therefore, the effect of ER from 0.96 to 1.26 was evaluated by altering the air flow. The value of ER directly influenced the measured temperature at different sections inside the combustor. Temperature profiles along the combustor corresponding to the steady state process are presented in Figure 3. The temperatures measured at different points were very sensitive to ER. Under the experimental conditions, the highest temperature was observed at the bottom of the combustor. The temperature gradually decreased across the reactor's height due to the heat loss across the wall. According to the above TGA analysis, most of the BMF volatiles evolved between 135 and 390°C, and generated most of the heat. Thus, the observed temperature peak was mainly due to the intense combustion of volatiles near the burner. Tarelho *et al.* (2011) and Al-Widyan *et al.* (2006) have reported similar results.

The temperatures of the different sections were very sensitive to ER. When the ER varied from 0.96 to 1.26, the temperatures of different sections synchronously increased and then decreased slightly. When the ER was 1.16, the BMF burned completely when enough oxygen was supplied, while the exhaust gas heat loss was

minimized. Thus, the temperature of different sections were simultaneously maximized. The combustion efficiency rose to 97.37%.

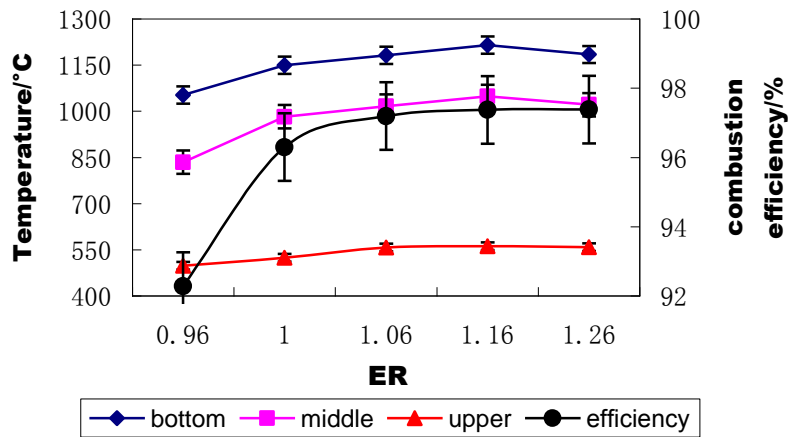


Fig. 3. Effect of ER on combustor temperature and combustion efficiency for pure biomass

Hence, the ER was fixed at 1.16 ± 0.04 throughout the series of co-firing tests, which corresponded with a flue gas O_2 level of about $3.0 \pm 0.2\%$ (dry). It may be readily noticed in Fig. 4 that the temperature profile of the combustor simultaneously increased when the coal blend ratio varied from 0 to 30 wt. %. A similar trend was reported with a 20 kW down-fired combustor (Munir *et al.* 2010b) and a short-combustion-chamber fluidized-bed combustor when increasing the coal blend ratios (Madhiyanon *et al.* 2011). Since coal has a higher carbon content and higher heating value when compared to biomass (*e.g.*, Table 1), small additions of coal may increase the heating value of fuel and increase the combustion temperature. The maximum temperature rose from 1215 to 1319°C when the coal blend ratio increased from 0 to 30%. In addition, the effect of the coal blend ratio on the bottom section temperature was much greater than that of the middle and the upper sections. This could be caused by the fact that coal is heavier than the biomass; coal particles tended to stay at the combustor bottom longer than the biomass. Therefore, as the coal blend ratio increased, so did the bottom temperature.

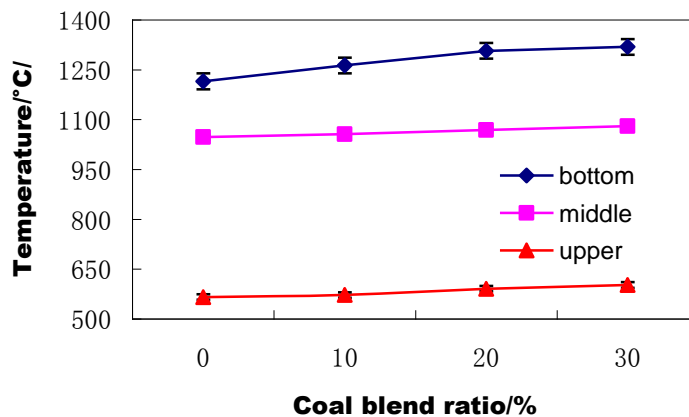


Fig. 4. Effect of coal blend ratio on combustor temperature for ER=1.16

The observed improvement leveled out as the coal blend ratio rose above 20%. This observation can be explained as follows. As the ER was 1.16, the temperature in the combustor was a result of two competitive effects: the flame intensity and the modest calorific value of the biomass. The Shazadeh and DeGroot expression (Tillman 2000) can be used to relate these two competing effects:

$$I_f = (dw/dt) \cdot h \quad (2)$$

where I_f is flame or reaction intensity, dw/dt is the weight loss with respect to time, measured by TGA, and h is the heat content of the fuel particle. The rapid weight loss of the biofuels when compared to any coal (shown in Fig. 2) offset the modest caloric value of biomass (Tillman 2000). This process of volatile release can be enhanced by using smaller particles. BMF ignites rapidly and supports earlier ignition of the entire mass of fuel in the furnace. Moreover, additional air is needed for coal combustion due to its lower oxygen content versus that of biomass. This results in more supply air that must be heated (Jenkins *et al.* 1998) along with more heated exhaust gas, representing a heat loss.

Analysis of Flue Gas

The flue gas compositions were measured for an ER of 1.16, and the results are shown in Fig. 5. It is intriguing that even though burning coal was inherently more difficult than burning ramie residue, the CO emissions diminished and the combustion efficiency was enhanced when increasing the coal fraction. This observation can be explained (Sathitruangsak *et al.* 2009), since the volatiles for the pure ramie residue combustion may be partially transformed subsequently into CO in the upper regions of the combustor and escape at the exit. Additionally, with higher coal content, the blend fuel liberated less volatiles near the top of the combustor, resulting in less CO being generated.

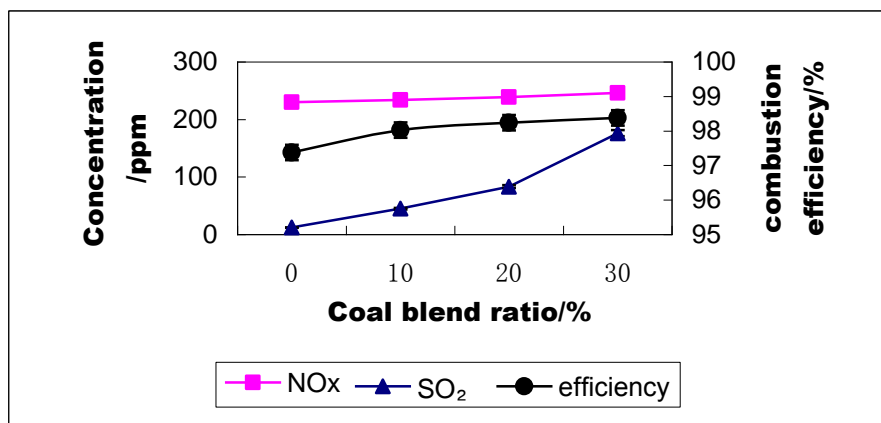


Fig. 5. Effect of coal blend ratio on SO₂ and NO_x emissions, and combustion efficiency for ER=1.16

As shown in Fig. 5, the NO_x emission only increased slightly with the increase in the proportion of coal in the blend, despite the high N content in the coal compared with the biomass. Previous studies virtually indicated that not only were the NO_x emissions dependent upon N-fuel content, but also on the operating conditions (*i.e.* excess air and combustor temperature) and the fuel characteristics (Gani *et al.* 2005; Skodras *et al.*

2002). Moreover, the dependence of SO₂ emissions on the coal fraction was shown in Fig. 5. As expected, increased SO₂ emissions were relative to increased coal blend ratio. However, the exhaust emissions complied well with air pollutant regulation requirements.

Fouling and Slagging

The ash of the biomass is more alkaline in nature, particularly with the sodium and potassium levels. Sodium and potassium lower the melting point of the ash, which may aggravate the fouling problems that can occur during combustion (Sami *et al.* 2001). All ash samples were collected on air-cooled probes in the furnace in order to evaluate the influence of co-firing biomass with coal on ash properties. The chemical compositions of ash samples obtained from the co-firing tests are partly presented in Table 2. Ash behavior and deposition tendencies were predicted through the use of empirical indices. These indices (Vamvuka and Kakaras 2011) are the alkali index and the base-to-acid ratio. The alkali index is given by the following expression:

$$AI = \frac{(\% \text{Na}_2\text{O} + \% \text{K}_2\text{O})_{\text{ash content}}}{LHV} \quad (3)$$

The alkali index (*AI*) expresses the quantity of alkali oxide in the fuel per unit of fuel energy (kg alkali/GJ). When the alkali index values are in the range 0.17 to 0.34 kg alkali/GJ, fouling or slagging is probable, whereas when values are greater than 0.34, fouling or slagging is virtually certain to occur (Dayton *et al.* 1999; Miles *et al.* 1996). The base-to-acid ratio is defined as (Vamvuka and Kakaras 2011),

$$R_{b/a} = \frac{\% (\text{Fe}_2\text{O}_3 + \text{CaO} + \text{MgO} + \text{K}_2\text{O} + \text{Na}_2\text{O})}{\% (\text{SiO}_2 + \text{TiO}_2 + \text{Al}_2\text{O}_3)} \quad (4)$$

where the label for each compound makes reference to its weight concentration in the ash. As the *R_{b/a}* value increases, the fouling tendency of a fuel ash increases. This ratio for biomass often exceeds 1.0 and may be beyond 2.0; *R_{b/a}* is usually lower than 1.0 in for coal (Tillman 2000). The base/acid ratio is an indication of fuel's performance in association with problematic deposit formations (Tillman 2000).

The calculation showed that increasing the coal blend ratio should result in less fouling and slagging, with a decrease in *AI* values (from 0.4 to 0.28) and decrease in *R_{b/a}* values (from 2.3 to 0.9). Coal blend ratio of 0 to 30% (mass basis) contributed to considerably low *AI* values. When the *AI* values varied from 0.4 to 0.28, the ash slagging/fouling tendencies changed from "certain slagging/fouling" to "probable slagging/fouling". This observation suggested that biomass co-firing with coal could mitigate the fouling and slagging tendencies due to the dilution and the consumption of alkali metals *via* the interactions with sulphur or/and silica in the coal (Zhang *et al.* 2010).

Table 2. Ash Chemical Composition of the Samples

Components (%)	SiO ₂	Al ₂ O ₃	Fe ₂ O ₃	MgO	K ₂ O	Na ₂ O	CaO	P ₂ O ₅	SO ₃	TiO ₂
BMF	14.28	3.16	2.38	7.14	8.10	6.40	42.82	4.80	2.91	2.91
Coal	45.58	30.02	9.69	—	2.02	—	5.48	0.85	4.34	1.64

CONCLUSIONS

1. The maximized temperature achieved with the cyclone furnace firing of only ramie residual biomass was 1215°C with an equivalence ratio (ER) of 1.16.
2. Coal additions to ramie residual biomass can improve the heating value of the fuel, as well as the combustion temperature, with low pollutant emissions. Increasing the coal fraction from 0 to 30 wt. % caused the peak temperatures rise to 1319°C along with improved combustion efficiency.
3. Co-firing ramie residue with coal seems more feasible than with ramie residue alone due to the potential risk of slagging and fouling of the latter.

ACKNOWLEDGMENTS

This research was supported by the National High Technology Research and Development Program (863 Program) of China (No. 2012AA101809). The authors are grateful to the Analytical and Testing Center of Huazhong University of Science and Technology for carrying out the ultimate analysis, the thermogravimetric analysis, and the ash properties analyses of the samples.

REFERENCES CITED

- Al-Widyan, M. I., Tashtoush, G., and Hamasha, A. M. (2006). "Combustion and emissions of pulverized olive cake in tube furnace," *Energy Convers. Manage.* 47(11-12), 1588-1596.
- Dai, J. J., and Grace, J. R. (2008). "Biomass screw feeding with tapered and extended sections," *Powder Technol.* 186(1), 56-64.
- Dayton, D. C., Jenkins, B. M., Turn, S. Q., Bakker, R. R., Williams, R. B., Belleoudry, D., and Hill, L. M. (1999). "Release of inorganic constituents from leached biomass during thermal conversion," *Energy Fuels* 13, 860-870.
- Gani, A., Morishita, K., Nishikawa, K., and Naruse, I. (2005). "Characteristics of co-combustion of low-rank coal with biomass," *Energy Fuels* 19(4), 1652-1659.
- Gil, M.V., Casal, D., Pevida, C., Pis, J. J., and Rubiera, F. (2010). "Thermal behaviour and kinetics of coal/biomass blends during co-combustion," *Bioresour. Technol.* 101(14), 5601-5608.
- Haykiri-Acma, H., and Yaman, S. (2008). "Effect of co-combustion on the burnout of lignite/biomass blends: A Turkish case study," *Waste Manage.* 28(11), 2077-2084.
- Jeguirim, M., Dorge, S., and Trouve, G. (2010). "Thermogravimetric analysis and emission characteristics of two energy crops in air atmosphere: *Arundo donax* and *Miscanthus giganthus*," *Bioresour. Technol.* 101(2), 788-793.
- Jenkins, B. M., Baxter, L. L., Miles Jr., T. R., and Miles, T. R. (1998). "Combustion properties of biomass," *Fuel Process. Technol.* 54(1-3), 17-46.

- Leckner, B. (2007). "Co-combustion – A summary of technology," *Therm. Sci.* 11(4), 5-40.
- Li, X. G., Lv, Y., Ma, B. G., Jian, S. W., and Tan, H. B. (2011). "Thermogravimetric investigation on co-combustion characteristics of tobacco residue and high-ash coal," *Bioresour. Technol.* 102(20), 9783-9787.
- Luo, S. Y., Xiao, B., Hu, Z. Q., Liu, S. M., and Guan, Y. W. (2009). "Experimental study on oxygen-enriched combustion of biomass micro fuel," *Energy* 34(11), 1880-1884.
- Luo, S. Y., Xiao, B., Hu, Z. Q., Liu, S. M., and He, M. Y. (2010). "Experimental study on combustion of biomass micron fuel (BMF) in cyclone furnace," *Energy Convers. Manage.* 51(11), 2098-2102.
- Madhiyanon, T., Sathitruangsak, P., and Soponronnarit, S. (2009). "Co-combustion of rice husk with coal in a cyclonic fluidized-bed combustor (ψ -FBC)," *Fuel* 88(1), 132-138.
- Madhiyanon, T., Sathitruangsak, P., and Soponronnarit, S. (2011). "Influences of coal size and coal-feeding location in co-firing with rice husks on performance of a short-combustion-chamber fluidized-bed combustor (SFBC)," *Fuel Process. Technol.* 92(3), 462-470.
- Miles, T. R., Miles Jr., T. R., Baxter, L. L., Bryers, R. W., Jenkins, B. M., and Oden, L. L. (1996). "Boiler deposits from firing biomass fuels," *Biomass Bioenergy* 10(2-3), 125-138.
- Munir, S., Daood, S. S., Nimmo, W., Cunliffe, A. M., and Gibbs, B. M. (2009). "Thermal analysis and devolatilization kinetics of cotton stalk, sugar cane, bagasse and shea meal under nitrogen and air atmospheres," *Bioresour. Technol.* 100, 1413-1418.
- Munir, S., Nimmo, W., and Gibbs, B. M. (2010a). "Shea meal and cotton stalk as potential fuels for co-combustion with coal," *Bioresour. Technol.* 101(3), 7614-7623.
- Munir, S., Nimmo, W., and Gibbs, B. M. (2010b). "Co-combustion of agricultural residues with coal: Turning waste into energy," *Energy Fuels* 24(3), 2146-2153.
- Munir, S., Nimmo, W., and Gibbs, B. M. (2011). "The effect of air staged, co-combustion of pulverised coal and biomass blends on NO_x emissions and combustion efficiency," *Fuel* 90(1), 126-135.
- Narayanan, K. V., and Natarajan, E. (2007). "Experimental studies on cofiring of coal and biomass blends in India," *Renew. Energ.* 32(15), 2549-2558.
- Sami, M., Annamalai, K., and Wooldridge, M. (2001). "Co-firing of coal and biomass fuel blends," *Progr. Energy Combust Sci.* 27(2), 7-23.
- Skodras, G., Grammelis, P., Samaras, P., Vourliotis, P., Kakaras, E., and Sakellariopoulos, G. P. (2002). "Emissions monitoring during coal waste wood co-combustion in an industrial steam boiler," *Fuel* 81(5), 547-54.
- Tarelho, L. A. C., Neves, D. S. F., and Matos, M. A. A. (2011). "Forest biomass waste combustion in a pilot-scale bubbling fluidized bed combustor," *Biomass Bioenergy* 35(4), 1511-1523.
- Tillman, D. A. (2000). "Biomass cofiring: The technology, the experience, the combustion consequences," *Biomass Bioenergy* 19(6), 365-384.
- Sathitruangsak, P., Madhiyanon, T., and Soponronnarit S. (2009). "Rice husk co-firing with coal in a short-combustion-chamber fluidized-bed combustor (SFBC)," *Fuel* 88(8), 1394-1402.

- Vamvuka, D., and Kakaras, E. (2011). "Ash properties and environmental impact of various biomass and coal fuels and their blends," *Fuel Process. Technol.* 92(3), 570-581.
- Wang, X., Tan, H., Niu, Y., Pourkashanian, M., Ma, L., Chen, E., Liu, Y., Liu, Z. and Xu, T. (2011). "Experimental investigation on biomass co-firing in a 300 MW pulverized coal-fired utility furnace in China," *P. Combust Inst.* 33(2), 2725-2733.
- Zhang, L. H., and Xu, C.B., (Charles), Champagne, P. (2010). "Overview of recent advances in thermo-chemical conversion of biomass," *Energy Convers. Manage.* 51(5), 969-982

Article submitted: October 10, 2012; Peer review completed: December 8, 2012; Revised version received: December 18, 2012; Accepted: December 19, 2012; Published: December 21, 2012.